10. D. W. Urry, *ibid.* **69**, 1610 (1972).
11. ———, *Jerusalem Symp. Quantum Chem. Biochem.* **5**, 723 (1973).
12. W. R. Veatch, E. T. Fossel, E. R. Blout, *Biochemistry* **13**, 5249 (1974).
13. W. R. Veatch and E. R. Blout, *ibid.*, p. 5257.
14. E. T. Fossel, W. R. Veatch, Yu. A. Ovchinnikov, E. R. Blout, *ibid.*, p. 5264.
15. D. W. Urry, M. M. Long, M. Jacobs, R. D. Harris, *Ann. N.Y. Acad. Sci.* **264**, 203 (1975).
16. H. J. Apel, E. Bamberg, H. Alpes, P. Lauger, *J. Membr. Biol.* **31**, 171 (1977).
17. E. Bamberg, H. J. Apel, H. Alpes, *Proc. Natl. Acad. Sci. U.S.A.* **74**, 2402 (1977).
18. D. W. Urry, *Ann. N.Y. Acad. Sci.*, in press.
19. R. J. Bradley, W. O. Romine, M. M. Long, T. Ohnishi, M. A. Jacobs, D. W. Urry, *Arch. Biochem. Biophys.* **178**, 468 (1977).
20. H. A. Kolb, P. Lauger, E. Bamberg, *J. Membr. Biol.* **20**, 133 (1975).
21. W. O. Romine, J. Sherrette, G. B. Brown, R. J. Bradley, *Biophys. J.* **17**, 269 (1977).
22. E. Bamberg, R. J. Bradley, D. W. Urry, in preparation.
23. Supported in part by NIH grants HL-11310 and GM-07195 and NSF grant BNS75-14321. We thank E. Bamberg for very helpful discussions on the structure of **3**.

3 October 1977; revised 11 January 1978

Potassium Activation Associated with Intraneuronal Free Calcium

Abstract. *Relations between calcium entry and activation of a calcium-dependent outward current during depolarization were examined under voltage clamp in dorid giant neurons injected with the calcium-sensitive photoprotein aequorin. Activation kinetics and amplitude of the slow calcium-dependent component were both found to be related to the rate and extent of free calcium accumulation and to the electromotive force acting on potassium ions, independent of the calcium activation kinetics. This indicates that the activation of the calcium-dependent outward current is more closely related to the transient intracellular accumulation of free calcium ions than to the movement of calcium through the plasma membrane during depolarization.*

A component of outward current carried by potassium ions and activated by the entry of calcium ions through the cell surface during membrane depolarization has been inferred from recent electrophysiological studies of excitable cells (*1–7*). The calcium-sensitive late outward current $I_{K(Ca)}$ has been implicated in a number of fundamental neurophysiological phenomena including the repolarization and undershoot that follow an action potential (*3, 8*) and the hyperpolarization that follows a train of action potentials or that terminates the pacemaker wave in spontaneously bursting neurons (*9, 10*). It is distinct from the other major late potassium current, namely the classical potential-activated, delayed rectifying current $I_{K(pot)}$ (*5*). Unlike $I_{K(Ca)}$, $I_{K(pot)}$ is both insensitive to extracellular calcium-blocking agents and is blocked selectively by tetraethylammonium ions injected into the cell (*5, 7a*).

To our knowledge, activation of the calcium-dependent outward current has not, until now, been directly correlated with intracellular Ca^{2+} accumulation during depolarization of the cell membrane. A role of Ca^{2+} in the activation of this current has been inferred, however, from the following: (i) intracellular injection of Ca^{2+} can produce increase in resting conductance to K^+ (*11*); (ii) Ca^{2+} entry continues during prolonged depolarization and trains of action potentials, and K^+ conductance remains transiently enhanced following such entry (*9, 10, 12–18*), decaying as the Ca^{2+} concentration returns to the resting level (*10, 14, 15*); (iii) delayed outward current plotted against membrane voltage V_m in voltage-clamp experiments exhibits a characteristic hump that imparts an N shape to the current-voltage (*I-V*) plot (*4, 7*). The hump is eliminated by procedures that interfere with Ca^{2+} entry (*4, 5*). Formation of a hump on the late *I-V* plot has been ascribed (*4–7*) to Ca^{2+} activation of $I_{K(Ca)}$ as follows. Entry of Ca^{2+} must pass through a maximum along the voltage axis determined by the relation $I_{Ca} = g_{Ca}(V_m - E_{Ca})$, with the calcium current I_{Ca} rising with membrane voltage until the conductance g_{Ca} levels off; it undergoes a progressive decline toward zero with further displacement of the membrane potential as V_m approaches the calcium equilibrium potential E_{Ca}.

We have used the calcium-sensitive photoprotein aequorin injected into voltage-clamped neurons to examine the activation of the outward current in relation to the transient accumulation of Ca^{2+} during its entry under membrane depolarization. The Ca^{2+} concentration transient recorded during depolarization was shown to be associated with two manifestations of a calcium-dependent outward current, namely (i) the hump of the N-shaped late *I-V* plot and (ii) a component of the outward-current trajectory exhibiting slow activation kinetics (*5*). The relation of outward current activation to the Ca^{2+} signal indicates that it is not activation of g_{Ca} or I_{Ca} but rather accumulation of Ca^{2+} on its entry that determines the activation of the outward current.

Giant neurons of the nudibranch *Anisodoris nobilis* were exposed and bathed in artificial seawater containing 470 m*M* NaCl, 10 m*M* $CaCl_2$, 10 m*M* KCl, 50 m*M* $MgCl_2$, 10 m*M* glucose, and 5 m*M* Hepes [4-(2-hydroxyethyl)-1-piperazineethanesulfonic acid; Sigma] at *p*H 7.7 and 15° ± 1°C. After KCl-filled current and voltage electrodes were inserted into the cells, the aequorin dissolved in 100 m*M* KCl plus 4 m*M* 2-{[tris(hydroxymethyl)-methyl]amino}ethanesulfonic acid (Sigma) at *p*H 6.8 was slowly injected under pressure. Only cells showing normal resting and action potentials, minimal input leakage, and a minimal background aequorin emission were used. The light emitted by the injected aequorin was monitored through a fiber optic wave guide with an EMI 9635A photomultiplier tube and displayed as the aequorin signal, along with voltage and membrane current, measured at the summing junction of the operational amplifier that held the bath at ground potential. Positive-going clamp pulses lasting 200 msec were presented at 30-second intervals. Recordings were taken 30 to 180 minutes after injection of the aequorin, which allowed sufficient time for diffusion of the photoprotein throughout the neuron soma. Some characteristics of the aequorin response in these cells and details of the methods are described elsewhere (*15*). The intensity of the aequorin emission was reported to be proportional to the second or even the third power of the free Ca^{2+} concentration (*19*). Thus, to approximate the voltage-dependent transient rise in Ca^{2+} concentration near the inner surface of the membrane, we plotted the square root of the aequorin signal–voltage curve (Fig. 1B), as done by Baker *et al.* (*20*).

The amplitude of the aequorin signal at the end of the 200-msec pulse (Fig. 1A) depended on pulse voltage, reaching a maximum in different cells at potentials ranging from 30 to 70 mV (*21*) and then subsiding with further increases in potential (Fig. 1B). In the square-root plot the falling limb was linear. This behavior is predicted for the rate of entry of Ca^{2+} (see above), which lends support to the use of the square root of the aequorin signal as an approximation to the transient free Ca^{2+} concentration, $[Ca]_i$, near the cytoplasmic surface of the plasma membrane. The voltage at which the signal was fully suppressed varied in different cells, but was characteristically above 100 mV. Some cells failed to ex-

0036-8075/78/0428-0437$00.50/0

hibit full suppression, with the signal curve flattening to a low level at high potentials. This may have been caused by poor isopotentiality of the excited region of membrane in those cells. Extensive surface infoldings, for example, could interfere with spatial uniformity of the clamp. An "off" response at the end of a high-voltage pulse, indicating additional entry of Ca^{2+} before calcium channels close, was not seen, which suggests rapid closing of these channels on repolarization. The aequorin-voltage relations in these cells are similar to those reported for squid axon (*21*).

The minimum of the N-shaped component of the late *I-V* plot coincided with the return to zero of the aequorin and square-root plots (Fig. 1B). This is predicted by the hypothesis that a component of K^+ conductance is activated as a consequence of Ca^{2+} entry during depolarization. The outward current at that potential is assumed to pass predominantly through potential-activated channels, since Ca^{2+} entry near E_{Ca} should be minimal.

Figure 1B shows a significant positive displacement of the membrane current maximum relative to aequorin signal maximum. Such displacements, which range up to 40 or 50 mV, are expected on the following grounds (Fig. 2). (i) When V_m exceeds the level at which g_{Ca} and concomitantly the calcium-activated potassium conductance $g_{K(Ca)}$ are fully activated, the electromotive force (EMF) acting on calcium ($V_m - E_{Ca}$) steadily declines as V_m approaches E_{Ca}, while the EMF acting on potassium ($V_m - E_K$) continues to rise. This will produce an arclike positive-going ballooning of the $I_{K(Ca)}$-voltage relation relative to the falling limb of the I_{Ca} plot. (ii) At voltages below the I_{Ca} maximum, the EMF acting on potassium diminishes with potential, producing a reduction in $I_{K(Ca)}$ relative to I_{Ca}. Because of this displacement, the charge-canceling effect of the inward calcium current on the outward potassium current is less significant at higher than at lower voltages, and this adds a further positive displacement to the net-current peak. The sum of these effects, namely that the plot of calcium-dependent net outward current becomes skewed toward more positive potentials relative to the $[Ca]_i$ curve, is illustrated in Fig. 2A. There is a further positive displacement due to summation with $I_{K(pot)}$ (Fig. 2B), so that the hump can be displaced as much as 50 mV relative to the aequorin signal maximum.

Figure 1A shows a relation between the size of the aequorin signal and the slowly rising component of the outward-current trajectory (*22*). This component, which develops more slowly than the rapidly rising component with which it sums, is illustrated in the superimposed tracings of Fig. 1C. It becomes smaller with the decline in the aequorin signal that occurs with increasing pulse voltage, and finally all but disappears when the aequorin signal becomes minimal or is absent (in this case at 140 mV). The current trajectory that remains is relatively flat after an initial small, rapid relaxation. Since the slow component becomes smaller with the decrease in aequorin signal that occurs as V_m approaches E_{Ca} (Fig. 1A) and is abolished by applications of cobalt (*5, 7*), it is identified as $I_{K(Ca)}$.

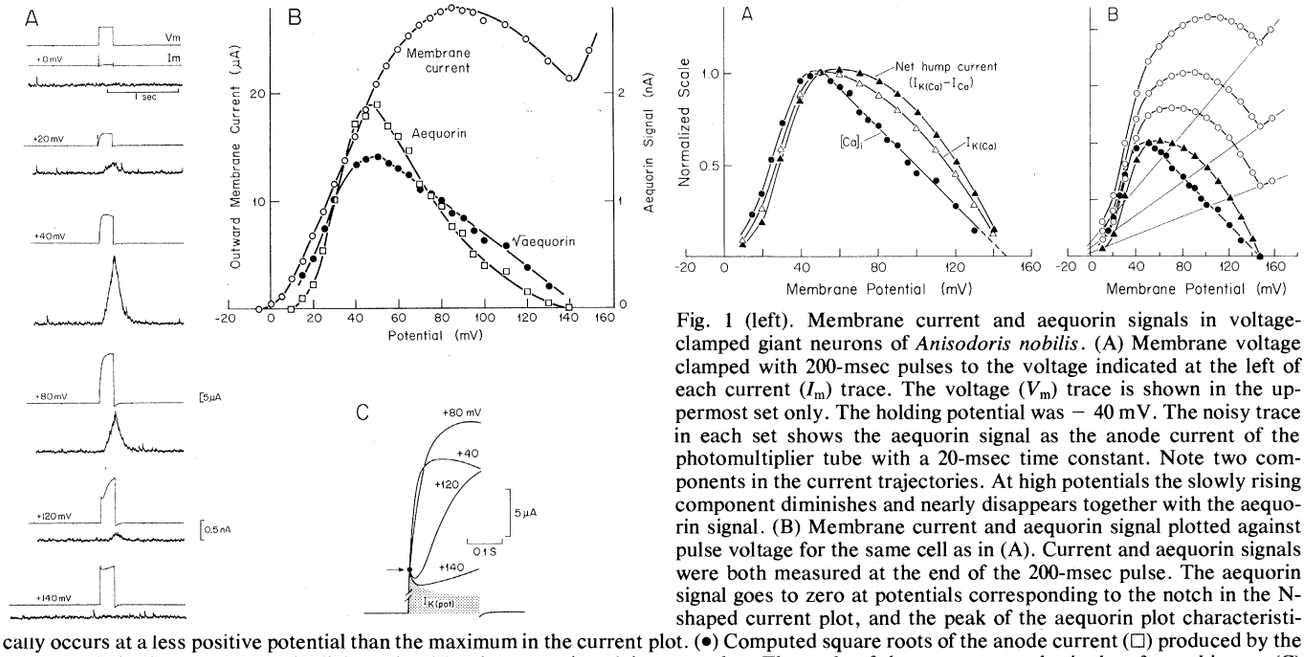

Fig. 1 (left). Membrane current and aequorin signals in voltage-clamped giant neurons of *Anisodoris nobilis*. (A) Membrane voltage clamped with 200-msec pulses to the voltage indicated at the left of each current (I_m) trace. The voltage (V_m) trace is shown in the uppermost set only. The holding potential was − 40 mV. The noisy trace in each set shows the aequorin signal as the anode current of the photomultiplier tube with a 20-msec time constant. Note two components in the current trajectories. At high potentials the slowly rising component diminishes and nearly disappears together with the aequorin signal. (B) Membrane current and aequorin signal plotted against pulse voltage for the same cell as in (A). Current and aequorin signals were both measured at the end of the 200-msec pulse. The aequorin signal goes to zero at potentials corresponding to the notch in the N-shaped current plot, and the peak of the aequorin plot characteristically occurs at a less positive potential than the maximum in the current plot. (•) Computed square roots of the anode current (□) produced by the photomultiplier in response to the light emitted by the aequorin-calcium complex. The scale of the square-root plot is therefore arbitrary. (C) Outward current trajectories for the potentials indicated, traced from (A). The starting points of the slow components (arrow) were aligned to the level from which they take off from the early peak of $I_{K(pot)}$ (stippled portion) (*3, 19*). The $I_{K(pot)}$ trajectory differs with potential and is shown approximately. Fig. 2 (right). Model depicting the origin of the net hump current and its positive displacement relative to the peak of the I_{Ca} activation curve. (A) The square root of the aequorin signal (•) from Fig. 1B is taken as an approximation of the calcium activity transient that occurs near the inner surface of the membrane, and therefore also as an approximation of I_{Ca} during positive displacement of the membrane potential. The assumptions are made that $g_{K(Ca)}$ is proportional to the calcium activity, that $I_{K(Ca)} = g_{K(Ca)}(V_m - E_K)$, and that $I_{K(Ca)} = 3\ I_{Ca}$ at 50 mV. The E_K was taken as − 70 mV. (△) Calculated $I_{K(Ca)}$ activation curve, and (▲) calculated net calcium-dependent current, $I_{K(Ca)} - I_{Ca}$. The plots are not to scale, but are all normalized to unity at 50 mV to facilitate comparison of their shapes. The increased driving force ($V_m - E_K$) acting on potassium with increasing positive clamp potential causes skewing of the $I_{K(Ca)}$ curve (△) toward more positive potentials relative to the $[Ca]_i$ and I_{Ca} curve (•). The short-circuiting action of I_{Ca} produces a further skewing of the calcium-dependent hump current (▲). (B) Summation of the hump current with three hypothetical $I_{K(pot)}$ activation curves (straight lines, each originating at −10 mV but representing a different range of conductance) produces three net outward current plots (○). With increasing slope of $I_{K(pot)}$, the hump maximum has a greater positive displacement. Deviations from the exact shape of the experimental *I-V* plot (Fig. 1B) may arise from simplifications or inaccuracies in the quantitative assumptions employed. Moreover, actual $I_{K(pot)}$ activation curves are not completely linear, but show an initial slow rise, becoming steeper at the higher potentials.

The kinetics of $I_{K(Ca)}$ provide insight into the manner of its activation. At 40 mV, calcium accumulation is rapid, but potassium is driven by a smaller EMF than it is at 80 mV. The result at 40 mV is (i) a fast rise in $I_{K(Ca)}$, consistent with rapid activation of $g_{K(Ca)}$ by rapid accumulation of Ca^{2+} near the inner surface of the membrane, and (ii) a smaller outward-current maximum than at 80 mV. In going from the peak of the $[Ca]_i$-voltage plot toward E_{Ca} (40 to 140 mV) the EMF acting on potassium increases while that acting on calcium decreases. Over this range the rate of entry and accumulation of Ca^{2+} progressively declines, as does the rate of activation of $I_{K(Ca)}$. Thus, although g_{Ca} and $V_m - E_K$ are high, and presumably g_{Ca} (and hence I_{Ca}) is activated rapidly at 120 and 140 mV, $g_{K(Ca)}$ is activated very slowly, more or less in parallel with the slow and weak rise in $[Ca]_i$ inferred from the aequorin signal at those potentials (Fig. 1A).

The observed agreement between the voltage dependence of a component of outward current and the voltage relations of Ca^{2+} entry that we detected with the aid of injected aequorin provides independent evidence in support of the hypothesis (*1*–*4*) that Ca^{2+} entry during depolarization leads to the activation of a calcium-dependent potassium current. The similarities between the activation kinetics of this current and the kinetics of intracellular free Ca^{2+} accumulation indicate that activation of $I_{K(Ca)}$ during depolarization is causally related to the intracellular concentration of free Ca^{2+} rather than to the passage of Ca^{2+} through the membrane (*23*)

ROGER ECKERT
DOUGLAS TILLOTSON
Department of Biology, University of California, Los Angeles 90024, and
Friday Harbor Laboratories, Friday Harbor, Washington 98250

References and Notes

1. K. Krnjević and A. Lisiewics, *J. Physiol. (London)* **225**, 363 (1972).
2. W. Clusin, D. Spray, M. V. L. Bennett, *Biol. Bull. (Woods Hole Mass.)* **147**, 472 (1974).
3. K. Krnjević, E. Puil, R. Werman, *Can. J. Physiol. Pharmacol.* **53**, 1214 (1975).
4. R. W. Meech and N. B. Standen, *J. Physiol. (London)* **249**, 211 (1975).
5. C. B. Heyer and H. D. Lux, *ibid.* **262**, 349 (1976); R. Eckert and H. D. Lux, *Science* **197**, 472 (1977).
6. W. T. Clusin and M. V. L. Bennett, *J. Gen. Physiol.* **69**, 145 (1977).
7. S. H. Thompson, *J. Physiol. (London)* **265**, 465 (1977).
7a. A. Hermann and A. L. F. Gorman, *Biophys. J.* **21**, 52a (1978).
8. R. W. Meech, *Comp. Biochem. Physiol. A* **48**, 397 (1974).
9. ———, *ibid.*, p. 387.
10. M. V. Thomas and A. L. F. Gorman, *Science* **196**, 531 (1977).
11. R. W. Meech, *J. Physiol. (London)* **237**, 259 (1974).
12. R. Eckert and H. D. Lux, *Brain Res.* **83**, 486 (1975).
13. ———, *J. Physiol. (London)* **254**, 129 (1976).
14. J. Stinnakre and L. Tauc, *Nature (London) New Biol.* **242**, 113 (1973).
15. R. Eckert, D. Tillotson, E. B. Ridgway, *Proc. Natl. Acad. Sci. U.S.A.* **74**, 1748 (1977).
16. M. S. Brodwick and D. Junge, *J. Physiol. (London)* **223**, 549 (1972).
17. D. Junge and C. L. Stephens, *ibid.* **235**, 155 (1973).
18. L. D. Partridge and C. F. Stevens, *ibid.* **256**, 315 (1976).
19. J. R. Blinks, F. G. Pendergast, D. G. Allen, *Pharmacol. Rev.* **28**, 1 (1976).
20. P. F. Baker, A. L. Hodgkin, E. B. Ridgway, *J. Physiol. (London)* **218**, 709 (1971). When the cube root of the aequorin signal was plotted against voltage, the falling limb was more convex.
21. We recorded no signals during 200- or 300-msec pulses going to − 10 mV or less, and usually not below 0 mV, even though Ca^{2+} currents have been detected at less positive potentials electrophysiologically in snail neurons (*12*, *13*), and optically in *Aplysia* by the arsenazo method (*10*). The small amount of Ca^{2+} that enters under small depolarizations may be rapidly bound to anionic sites, producing little buildup of $[Ca]_i$. Since the aequorin reacts only with free Ca^{2+}, rapidly bound Ca^{2+} would produce little light emission. This may also explain the latency between onset of depolarization and onset of the aequorin signal (Fig. 1A). Because of the power relation between Ca^{2+} concentration and aequorin emission (*19*) the aequorin method should be most sensitive to $[Ca]_i$ transients near the inner surface of the membrane, where Ca^{2+} is most concentrated during its entry before becoming dissipated by diffusion and removed by sequestering mechanisms.
22. It should not be overlooked that the net current trajectory must depart somewhat from the trajectory of potassium outward current, because a slow inward current sums algebraically with the late outward current [H. D. Lux and R. Eckert, *Nature (London)* **250**, 574 (1974)].
23. The intracellular accumulation of calcium in some neurons leads to a secondary effect, namely the desensitization or depression of $g_{K(Ca)}$ during subsequent depolarization (*5*).
24. We thank E. B. Ridgway for advice and help with the aequorin technique and for the use of essential items of equipment. We are grateful to E. B. Ridgway, O. Shimomura, and F. H. Johnson for the gift of purified aequorin, to T. Eckert for collecting specimens, and to the director and staff of Friday Harbor Laboratories of the University of Washington for providing space and facilities. Supported by PHS grants NS 8364, S07 RR07009, and GM 7191 and by NSF grant BMS 19464.

12 December 1977; revised 1 February 1978

Induction of Stalk and Spore Cell Differentiation by Cyclic AMP in Slugs of *Dictyostelium discoideum*

Abstract. *Multicellular masses of the cellular slime mold* Dictyostelium discoideum, *under conditions which ordinarily suppress cell differentiation, develop clusters of stalk cells and spore cells when implanted with Sephadex particles that had been soaked in* 5×10^{-3} M *cyclic adenosine monophosphate (AMP). A possible relation exists between oxygen gradients, cyclic AMP gradients, and the pattern of morphogenesis and cell differentiation during fruiting.*

The developmental program of *Dictyostelium discoideum*, and that of most other members of the group Acrasiales (cellular slime molds or social amoebas), includes the differentiation of two distinct cell types: thick-walled, vacuolated stalk cells and elliptical, encapsulated spore cells (*1*). Adenosine 3′,5′-monophosphate (cyclic AMP) has been identified as the chemotactic agent during the aggregation phase of the *D. discoideum* life cycle (*2*). This substance is also present in the migrating multicellular mass, the slug or pseudoplasmodium, in which prespore and prestalk regions are established. The concentration of bound cyclic AMP is highest at the anterior end of the slug, which is the region in which prestalk cells are localized (*3*). During fruiting body formation, these prestalk cells differentiate into mature stalk cells. A rise in extracellular cyclic AMP, with no increase in the level of intracellular cyclic AMP, has been reported at the time of fruiting (*4*). Bonner (*5*) demonstrated that exposure to $10^{-3}M$ cyclic AMP can cause isolated postvegetative amoebas or groups of amoebas to differentiate into stalk cells without involvement in fruiting body formation. A mutant strain (P-4) of *D. discoideum* undergoes up to 100 percent stalk cell differentiation when exposed to $10^{-4}M$ or $10^{-5}M$ cyclic AMP in 1 percent Bonner's salt solution (*6*). Thus, it is reasonable to hypothesize that cyclic AMP may be the normal control agent in stalk cell differentiation (*5*) and may in some way be involved in spore cell differentiation as well. Such a hypothesis asserts a "first messenger" role for cyclic AMP in the control of differentiation comparable to its role during the earlier aggregation stage.

As one test of this hypothesis, we decided to suppress fruiting and then implant sources of cyclic AMP into the suppressed slugs. We took advantage of the fact that slugs are prevented from fruiting when submerged in water (*7*). *Dictyostelium discoideum* NC-4 was maintained in two-membered culture with *Escherichia coli* B/r (*8*) and slugs were obtained on moist 2 percent nonnutrient agar surfaces by seeding mounds of *E. coli* with *D. discoideum* spores. After about 48 hours in darkness at 21°C, slugs migrated away from the mounds. Particles of Sephadex (G-50, fine, Pharmacia Fine Chemicals) were soaked in $5 \times 10^{-3}M$ cyclic AMP, collected by centrifugation, and dried overnight at room temperature in a hood. For each implantation, a particle was picked up on the

0036-8075/78/0428-0439$00.50/0